Ultrasonic and Optical Investigation of Mercury Content Influence on Metrological Properties of Reference Alloy Materials

Mirham A. Y. Barakat [1*], A. W. Abdallah [2]

[1] Ultrasonic, National Institute of Standards, (NIS)
[2] Line & End Secondary Standard., National Institute of Standards, (NIS)
*Corresponding author's email: mirham.barakat@nis.sci.eg

Article Type: Research article.
Received: 4 Sep 2023 **Accepted: 5 Sep 2023**

Abstract

Alloys are a mixture of pure metals. They had to be checked for their quality, production, and performance repeatability according to a standard. Thus, reference material may be obtained. The key novelty of this work is the preparation of a reference non- ferrous alloy material according to standards. It has great importance in the restorative materials. In addition, a novel ultrasonic technique was developed. Poly-methyl-methacrylate delay line was designed to modify the used ultrasonic transducers. Alloy powder of platinum modified non-gamma 2 mixed with different mercury percentages (0.5%, 1%, 1.5%, 2%, 2.5% and 3% weight by weight) at room temperature. According to standards, ultrasonic and optical measurements studied the influence of different levels of mercury in the alloy specimens. Ultrasonic velocities and attenuation measurements were carried out using the pulse echo technique. Ultrasonic velocities served to calculate the elastic properties, then to determine the mechanical behavior of the mixed alloy. Ultrasonic attenuation revealed the microstructure change of the mixed alloy. The number of crosslink density and the ultrasonic viscosity are measured. The changes in the optical constants, absorption coefficient, optical band gap, and Urbach energy were measured using the ellipsometric method. Results showed that the mercury content had a great influence on the mechanical properties and the microstructure of the alloys. In addition, 1, 1.5, and 2.5 % W/W mixed alloys were the most mixture that had homogeneous microstructure and could be used as reference restorative materials. The optimum one was the specimen with a mercury content of 2.5 %.

Keywords: Ultrasonics; Modified Transducers; Optics.

1 Introduction

Metal alloys are classified into two categories, ferrous and nonferrous. Different steels thus fall into the first category, and other popular alloys like brass, bronze, invar, etc. fall into the second

category. However, any alloy or any material for that matter has to be checked for its quality, production, and performance repeatability, and thus a standardization protocol is necessary. Many of the properties of such alloys are dependent on different crystalline phases of the individual metals when they are mixed. In order to achieve repeatability in their preparation process, all of their properties need to be standardized, i.e., measured, quantified, and catalogued. Such a process will result in production of standard alloys or certified reference materials. Thus, different national metrology institutes all over the world have been working on standardizing different alloys of their interest for growth of their own economies [1].

Amalgam is a metallic alloy formed by a reaction between mercury and an alloy in powder form containing silver, tin, copper, zinc, etc. with a very complex metallurgical structure. The alloy made from elements such as Ag, Sn, Cu and Pt, can be considered as biomaterials used as restorative material. This alloy was mixed with mercury to form mercury amalgams, which were used in dentistry because they were cheap, easy to use, durable, and safe. About 47% of all dentists still place mercury amalgam fillings. Therefore, the study of their physical, optical, and mechanical properties is very important. Mercury in silver amalgam forms a typical alloy that has approximately similar atomic radii of metals, so that one type of metal atom can replace another one without serious disruption of the crystal structure [2-3].

From the velocity of longitudinal and shear waves, the elastic moduli of the materials can be determined. Generally, elastic moduli are related to interatomic changes, fracture, porosity, crystal growth, etc. In addition, the elastic moduli of a material are important for understanding its mechanical behaviour. The ultrasonic attenuation is the intensity of the ultrasonic wave that decreases with the distance from the source during the propagation through the medium. It can be defined as the energy loss in the medium. The change in both the physical properties and microstructure of the medium is the main cause of this energy loss [4].

The influence of mercury content in amalgam has been investigated regarding its safety in the human mouth. Generally, most people have measurable but small amounts of mercury in their bodies. Even swallowing metallic mercury from a broken thermometer, a dental amalgam preparation, or pieces of an amalgam filling would not cause mercury poisoning. In contrast, breathing in large amounts of metallic mercury vapour can cause poisoning or adverse effects in the brain and kidneys, but low levels of mercury cannot be dangerous [5-6].

Studies have declared that mercury is used to bind the alloy particles together into a strong, durable, and solid filling. Mercury's unique properties (it is a liquid at room temperature and bonds well with the alloy powder) make it an important component of dental amalgam that contributes to its durability. Mercury content may have an influence on the amalgam properties. Thus, the restored teeth would have different characteristics [7-8].

The optical properties could be determined using the spectroscopic ellipsometer, which is a non-contact technique [9]. It measures the change that occurs in the polarization state of light upon reflection from the material surface. This change occurs due to the nature of the material under test. The general ellipsometry equation is as follows [10]:

$$\rho = \tan\psi \; e^{i\Delta} \qquad (1)$$

where ρ is the complex reflectance ratio, Ψ and Δ are the ellipsometric parameters, the change in amplitude and change in phase after reflection respectively.

From the ellipsometric parameters, the change in the optical properties due to the different mercury content in the mixed alloy materials was extracted. The optical properties are the optical constants (refractive index n and the extinction coefficient k), the surface roughness, the absorption coefficient, the optical band gap, the porosity, and the Urbach energy [11].
The aims of this study are the preparation of typical homogeneous alloys and the innovation of a novel ultrasonic technique. The homogeneous alloys are the mercury-amalgam alloys, which have challenging properties can be used in many applications like the fabrication of restorative materials. Their properties are measured, quantified and recorded to be used as reference restorative materials in the future. In addition, the novel ultrasonic technique is the modification of an ultrasonic transducer to improve the testing method. Ultrasonic and optical measurements were performed to evaluate the influence of the mercury content on the alloy properties.

2 Research Methodology

2.1 Materials preparation

According to ISO 24234:2021, cuboid specimens were prepared [12]. The specimens were prepared using an alloy powder from platinum modified non-gamma 2 alloy (60.10% Ag, 28.05% Sn, 11.80% Cu, and 0.05% Pt) and mercury (Southern Dental Industries LTD E4107 Australia). Amalgamator apparatus (DMG 410/1, De Lab, GmbH) mixed them for 17s, with mercury concentrations ratios of 0.5%, 1%, 1.5%, 2%, 2.5% and 3% weight by weight (W/W%). The wet mixtures were putted in a mold made from Plexiglas. The mixtures were left to dry and harden for 1 day in room temperature. The prepared specimens are cuboid of dimensions 12*14*15 mm^3 (Figure 1).

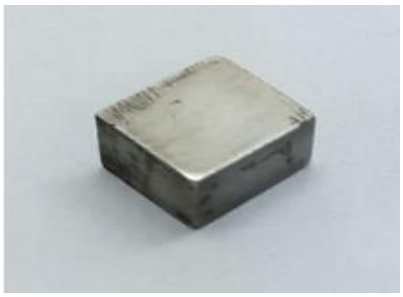

Figure 1: Example of the prepared alloy specimen.

2.2 Ultrasonic method

2.2.1 Mode of operation

Pulse echo technique is the used ultrasonic mode of operation following the ASTM standard (ASTM E114-15, 2015 [13]) by direct contact transducers. A longitudinal ultrasonic transducer of 2 MHz (S12HB2, Karl Deutsch) and a shear ultrasonic transducer of 2 MHz (B2S-Krautkramer) were used. An ultrasonic flaw detector (USN60, GE inspection technologies) was at A-scan display and gave distance/amplitude information. An oscilloscope (LeCroy W, wave Jet 354A) displayed the time/amplitude of the echoes. Standard blocks (VI and VII) used as reference test blocks to calibrate thickness measurements. The measurements were carried out in ambient room temperature of 24 ^{0}C ± 10 ^{0}C and relative humidity 47 % ± 5 %.

2.2.2 Modification of ultrasonic transducer

Delay lines of cube shape was designed to modify normal ultrasonic transducer of 2 MHz frequency. They were made from poly-methyl-methacrylate material (PMMA). They had considerably low acoustic impedance (Z) compared to those of the transducer and the specimens, to allow the passage of most beam energy. The acoustic impedance of PMMA is 3.26 MRayl [14], while that of the transducer is about 36.15 MRayl [15]. The acoustic impedance (Z) of the prepared alloy specimens ranged from about 14 to 23.7 MRayl depending on the mercury content (see section 3.1.4). The transducer near field (NF) is one of the important factors that can reflect the amelioration of the used transducers after using delay line. If the NF becomes smaller, the transducer's sensitivity becomes higher. NF is given by the following formula [16], Table 1:

$$NF = 4D_{eff}^2 f_0 C \qquad (2)$$

Where: D_{eff} is the transducer's effective diameter, f_0 is the operating frequency of the used transducer and C is the ultrasonic velocity in the prepared alloy specimens.

Table 1: *Near Field (NF) for the used transducers.*

Specimen according to Hg content	NF of normal transducer (S12HB2), mm		NF of shear transducer (B2S), mm	
	Before using DL	After using DL	Before using DL	After using DL
0.5 %	15.027	7.47274	7.89302	3.93302
1 %	15.0849	7.53062	7.98707	4.02707
1.5 %	15.3478	7.79357	8.49114	4.53114
2 %	15.7599	8.2057	8.99417	5.03417
2.5 %	16.4004	8.84621	9.77987	5.81987
3 %	17.2259	9.67162	10.8193	6.8593

From Table 1, the presence of a delay line caused a reduction in the near field of the used transducers by about 48 %. Thus, the used transducers – with delay line – became more sensitive to capture echoes easily from the specimens (Figure 2).

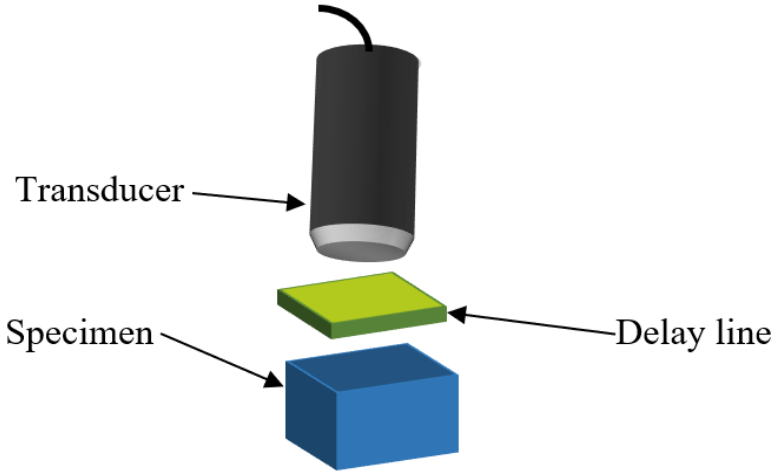

Figure 2: Sketch of ultrasonic measurement technique using delay line.

2.3 Density measurement

The density of the prepared EPDM composites was measured directly using a digital electronic balance with a density determination kit; B150536815; Model MS2045; Mettler Toledo, Switzerland.

2.4 Optical method

Ellipsometric measurements were conducted at room temperature using a spectroscopic ellipsometer type PHE-103 (Angstrom Advanced Inc.), as shown in Figure 3. A white light source passes through a linear polarizer and is then incident on the surface under test at a definite angle of incidence. The light is reflected from the surface and then passed through a quarter wave plate, a second linear polarizer and a detector [17]. The mixed alloy was measured in the spectral range from 300 nm -1000 nm and at an angle of incidence of 75º. The ellipsometric parameters of the alloys were extracted, and then the optical properties were obtained using the fitting process and mathematical modelling [18].

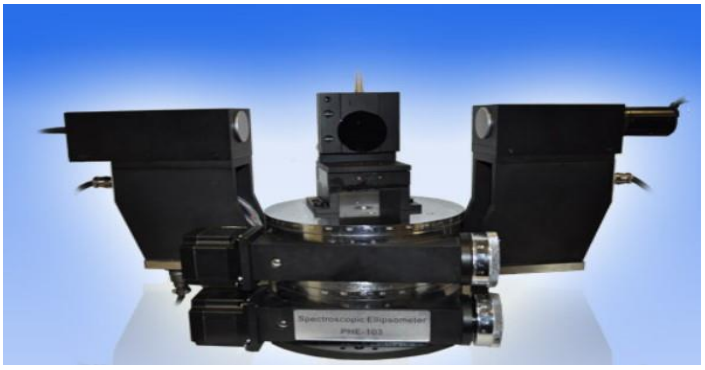

Figure 3: PHE-103 Spectroscopic Ellipsometer.

3 Results and Discussion

3.1 Ultrasonic measurements

Alloys are improved by mixing the metals with mercury. The desired performance is achieved depending on the homogeneity of the alloy's composition. Ultrasonic was used to determine the structure and properties of the alloy specimens. Ultrasonic velocity and attenuation are the two key factors in ultrasonic testing. The ultrasonic velocity and the density are used to compute the elastic modulus, Poisson's ratio and the crosslink density. The structure of the alloy specimens has a considerable impact on the attenuation. As a result, ultrasonic testing provides an easy, economical, and effective method for assessing the homogeneity of the alloy composition.

3.1.1 Ultrasonic velocity

Ultrasonic velocity gives information about alloy structure and composition. Compressional waves are the longitudinal velocity of an ultrasonic wave. Regarding wavelength, it mostly depends on specimen geometry. The relationship between the velocity (C) and the wavelength (λ) is direct: λ= C/frequency. The velocity that is most frequently measured in a lab; it clearly relates to a material's elastic characteristics.

Transverse waves are shear ultrasonic waves. Compared to longitudinal ones, they are more challenging to create with transducers. Since the shear velocity is almost half that of longitudinal waves at a given frequency. Any material that supports a shear wave will often support a longitudinal wave.

Ultrasonic velocities (Longitudinal, C_L and shear, C_s), were determined [19] according to the following formula, Figure 4.

$$C = \frac{2x}{t} \tag{3}$$

Where: C is the ultrasonic velocity, x is the thickness of the specimen and t is the time travelled by the echoes.

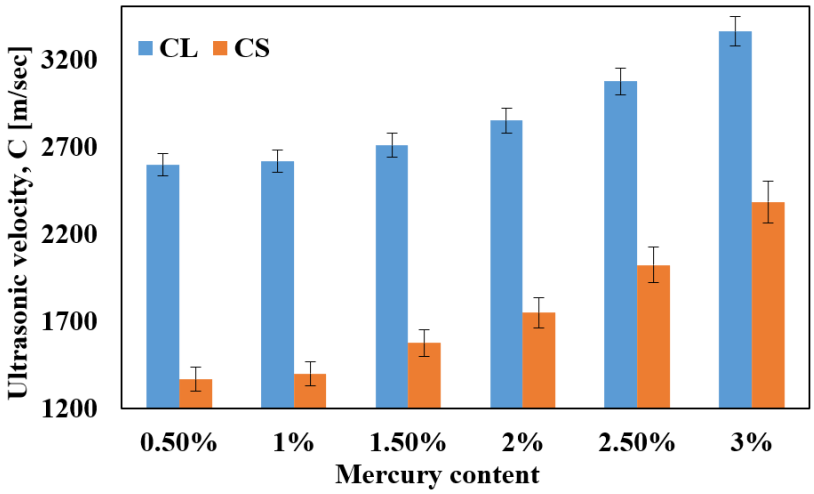

Figure 4: The ultrasonic velocities of the different alloy specimens.

From Figure 4, the ultrasonic longitudinal and shear velocities increased as the mercury content increased in the alloy's specimens. An amalgam is an alloy of mercury with another metal. It may be a liquid, a soft paste or a solid, depending on the proportion of mercury. One of the most important features of mercury concerns the formation of metallic bonding with the electrostatic attractive force of the conduction electrons. These electrons are formed in the alloy structure and they work to bind all the positively charged metal ions

together into a crystal lattice structure. Mercury promoted conductivity in the alloy material [20]. Therefore, increasing the mercury content may cause the promotion of wave transmission through the alloy material leading to decreasing the time of waves' travelling, then increasing the wave velocity. By adding mercury to the alloy specimens we obtained homogeneous mixture alloy of impact structure, especially that containing high mercury content (1.5, 2, 2.5, and 3 %). So, these alloy mixtures could be used as effective restorative materials that are homogeneous without gaps or defects. They could be challenged reference restorative materials.

3.1.2 Mechanical properties by ultrasonic

Ultrasonic measurements were used to study the mechanical properties and characterization of the prepared alloy specimens. The ultrasonic longitudinal and shear velocities (C_L and C_S) usually have a definite relationship to the elastic properties of the material, Poisson's ratio, and micro-hardness (Figures 5, 6, and 7). Therefore, Poisson's ratio (v), elastic moduli (E, L, G, K) and micro-hardness can be calculated from the following equations [**Error! Bookmark not defined.**21-22]:

$$v = \frac{1-2(C_S/C_L)^2}{2-2(C_S/C_L)^2} \quad (4)$$

$$E = 2\rho(C_S)^2(1+v) \quad (5)$$

$$L = \rho(C_L)^2 \quad (6)$$

$$G = \rho(C_S)^2 \quad (7)$$

$$K = L - [(4/3)G] \quad (8)$$

$$H = [(1-2v)E/(6(1+v)] \quad (9)$$

Where: v is the Poisson's ratio, ρ is the alloy density, E is the young's modulus, L is the longitudinal modulus, G is the shear modulus, K is the bulk modulus, and H is the micro-hardness.

By definition, Poisson's ratio measures the material's deformation in a perpendicular direction to that of the applied force. Generally, Poisson's ratio is dimensionless and ranges between 0.1 and 0.45. It differs according to the nature and structure of the material. It is also helpful in distinguishing ductile from brittle behaviour beyond the elastic limit [23]. The presence of the structural rearrangements induced a more compact atomic structure in the alloy as a function of mercury increasing content. Mercury promoted highly interconnected atoms. Therefore, the Poisson's ratio increased as mercury content increases in the alloy specimens (Figure 5).

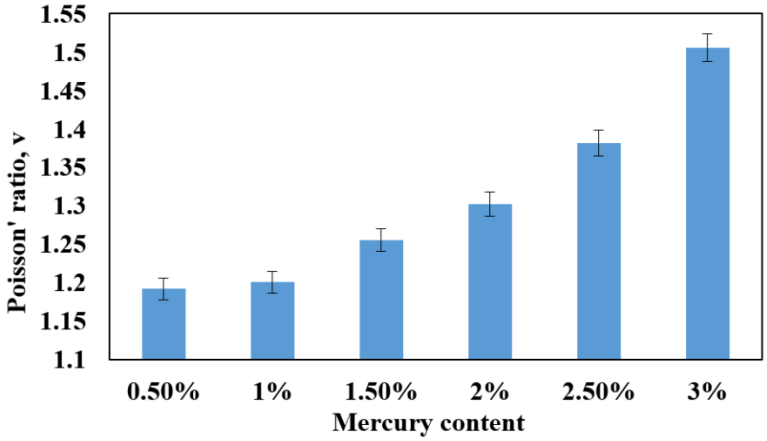

Figure 5: The Poisson's ratio of the different alloy specimens.

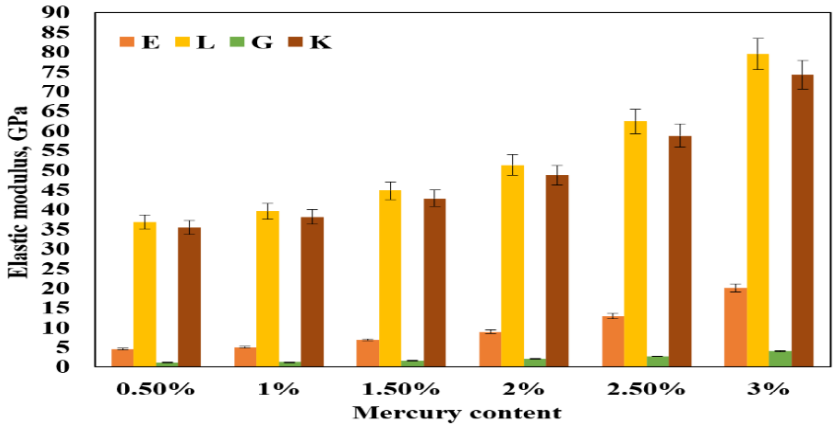

Figure 6: The elastic modulus of the different alloy specimens.

From Figure 6, the elastic moduli (E, L, G, and K) were increased with the increment of mercury content in the alloy specimens. From these findings, we can say that the nanoparticles of mercury enhanced the microstructure of the alloy specimens, they were arranged properly in the alloy structure and they didn't cause damage nor cracks [24]. They reinforced the alloy specimens. Alloy specimens that have 3 % of mercury showed the highest elastic moduli (E, L, G, and K) values. Therefore, we can say that the prepared alloy specimens had effective mechanical properties, which deduces that the choice of their content was effective. In addition, these materials had challenging mechanical properties to be used in many other applications that needed enhanced mechanical properties.

The micro-hardness (H) describes the rigidity of the material, the intermolecular bond strength and the uniform arrangement of molecules in the materials' structure, Figure 7. It can be calculated after knowing the Poisson's ratio (v) and the Young's modulus (E) [**Error! Bookmark not defined.**] (Eq. 9).

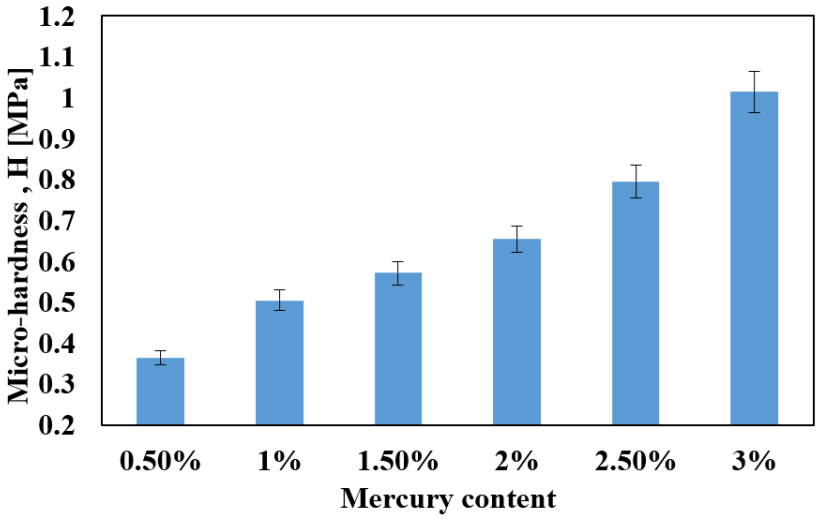

Figure 7: The micro-hardness of the different alloy specimens.

As shown in Figure 7, the micro-hardness (H) increased with the increment in mercury content within the alloy structure. The alloy specimens of 3 % mercury content showed the highest H value (about 1 MPa). The mercury particles caused a rigidity increment, high intermolecular strength, and uniform molecular distribution. Thus, the prepared alloys fulfilled the required properties to be good restorative materials.

3.1.3 Ultrasonic attenuation coefficient

Ultrasonic beams, like the other energy types, attenuate when passing through different media. The ultrasonic attenuation coefficient (α) is expressed as the amount of ultrasonic beam attenuation per unit length, and it usually notes the energy loss, which may arise from the microstructure of the material, porosity, impurities, defects, heat treatment, etc.

The ultrasonic attenuation coefficient is determined by the amplitude decay of a back-wall echo sequence. As per two successive echoes height (l_1 and l_2) measurements; the ultrasonic attenuation coefficient (α) was measured in dB/cm with respect to the path length ($x_2 - x_1$) [25], Fig. 8.

$$\alpha = (({}^{1}/_{(x_2 - x_1)})(\ln({}^{l_1}/_{l_2}) \quad (10)$$

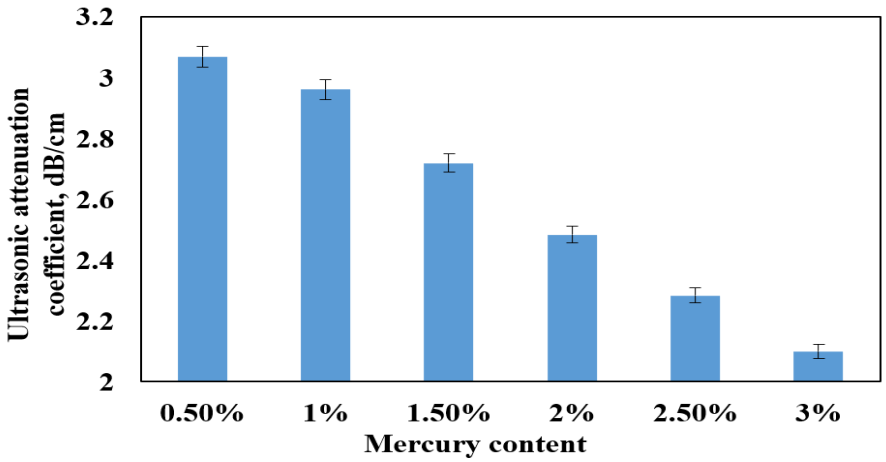

Figure 8: The ultrasonic attenuation coefficient of the different alloy specimens with respect to mercury content.

Figure 8 shows the decrement of the ultrasonic attenuation coefficient (α) with the increment of mercury content; the highest value was recorded for alloys of 0.5 % mercury, while the lowest one was for alloys containing 3 % of mercury. The decrement of ultrasonic attenuation coefficient is the best indicator that the mercury particles reduced dislocation and damage, but improved the alloy's structure [26]. Therefore, mercury can be regarded as a good binding material that performed good atoms bonding between metals in the alloy.

3.1.4 Ultrasonic acoustic impedance

The acoustic impedance (Z) depends on the ultrasonic velocity (C) and the materials' density (ρ). It describes how much resistance an ultrasound beam encounters as it passes through a material [27]. It is given by the following formula (Figure 10):

$$Z = \rho C \qquad (11)$$

The alloy specimens' density represented in Figure 9.

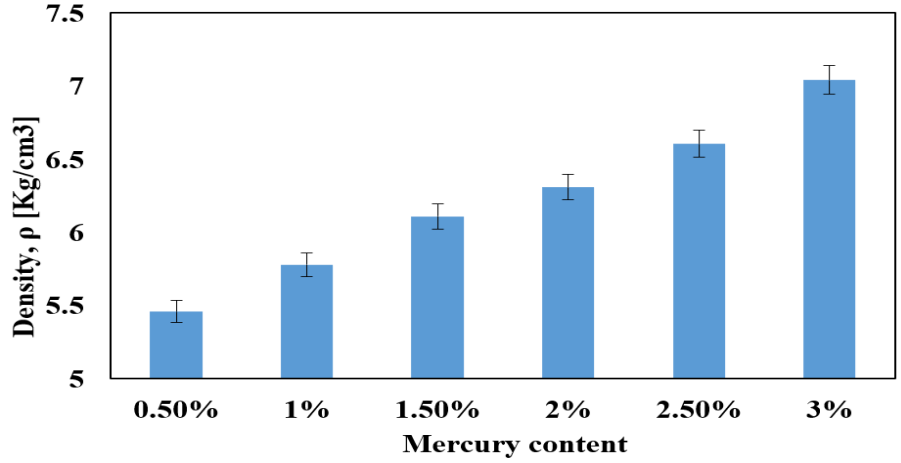

Figure 9: Density of different alloy specimens.

From Figure 9, the density increased as per the mercury content increment. Mercury material can be regarded as a binding agent for the metals in the alloy specimens. The mercury content increment caused more increment in the binding intermolecular force and in density [**28**].

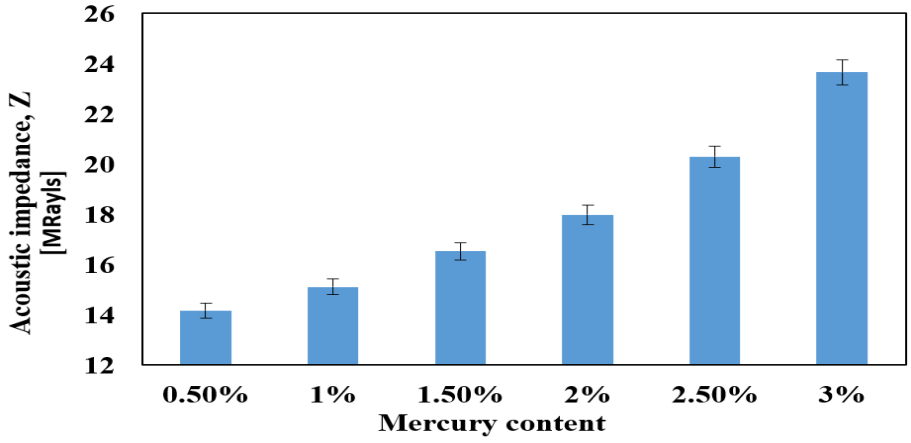

Figure 10: Acoustic impedance of alloy specimens with different mercury content.

From Figure 10, we noticed a remarkable increase in the acoustic impedance (Z) with the increment of mercury content in the alloy specimens. As mentioned in the formula of Z (Eq.

11), there is a direct relationship between Z and both density and ultrasonic velocity. The alloy's density and the ultrasonic velocity increased with the increase in the mercury content, as did the acoustic impedance. The increment in acoustic impedance (Z) clarified the increment in the micro-hardness of the alloy. This increment is good for performing good restorative materials that sustain strength and load.

3.1.5 The number of crosslink density (n_c)

The number of crosslink density, n_c is an important measured property that reveals the effect of mercury content on the alloys' microstructure (Figure 11). It is related to Poisson's ratio theoretically as follows:

$$n_c^{-\frac{1}{4}} = \frac{v}{0.28} \qquad (12)$$

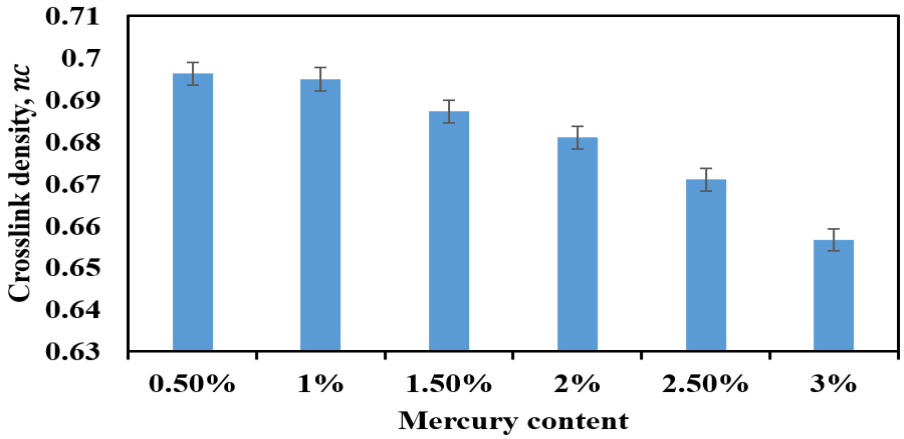

Figure 11: The crosslink density of the different alloy specimens.

From Figure 11, the crosslink density, n_c decreased with the increment of the mercury % content. Mercury ions occupy the interstitial space, thus the alloy's structure become more compact. The interatomic separation decreased with increment in mercury ions, which indicated the appearance of the stretching force. As a result, the crosslink density decreased as the percentage of mercury increased [29]. This could be a useful proof that assure the homogeneity of the prepared alloy specimens.

3.1.6 The ultrasonic viscosity (η_{us})

The viscosity is one of the most established methods to determine and proof compatibility of liquid metals and alloy. Many methods can determine viscosity, but the ultrasonic technique is the most useful one [30]

The prepared alloy specimens were measured before being solidified; they were liquid. The ultrasound viscosity technique is based on the velocity and attenuation measurements of an ultrasonic wave propagating in the liquid alloy. To measure ultrasonic viscosity (η_{us}), a system was developed. It consisted of two thin buffer plates from stainless steel and two transducers of same frequency (2 MHz), one transducer acted as a wave transmitter within the liquid alloy while the other one received waves reflected from the liquid alloy, Figure 12. The buffer plates protect the transducers' front from the sticky liquid alloy, which is tested during the mixing

process. Therefore, they avoid direct contact of the transducers and the liquid alloy. The buffer rods are square plates (1*20 mm^2). Their thickness is less than the near field (NF) of the 2 MHz transducer. The calculated near field ranged from about 4 to 17 mm (Table 1). Therefore, the buffer plates don't affect the measurements because they are within the near field region of the transducer.

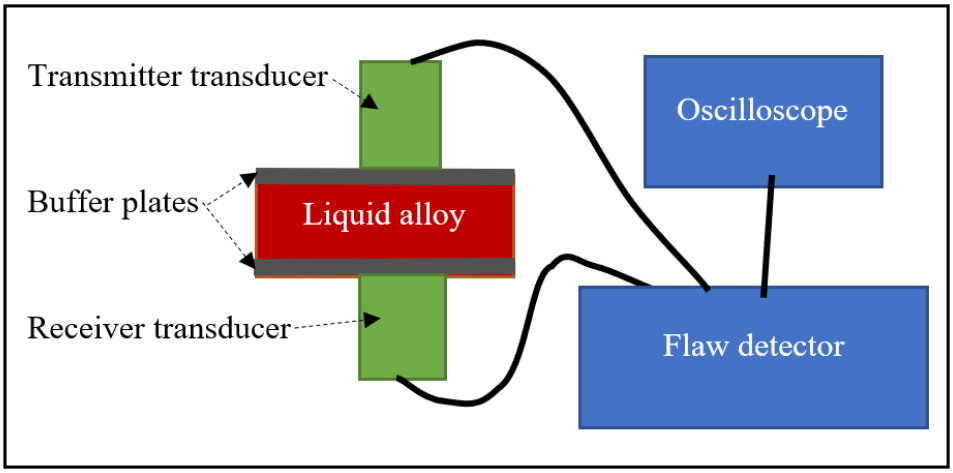

Figure 12: Sketch of the ultrasonic viscosity measuring system.

The liquid alloy, between the two buffer rods, has a thickness of 30 mm. The weight of the transducer represents the constant pressure on the buffer rods and the liquid alloy during the measurement. The ultrasound velocity (C_L) is found from the liquid alloy thickness (x), and the measured time (t) (Eq. 1) at the same time, the attenuation (α) is calculated from the ratio of the amplitudes of successive echoes and usually is given in dB/cm (Eq. 10). Then the ultrasonic viscosity (η_{us}) is calculated [31], Figure 13:

$$\eta_{us} = \frac{2\rho\,\alpha\,C_l^3}{\omega^2} \qquad (13)$$

where ρ is the density and ω is the angular frequency ($\omega = 2\pi f_0$).

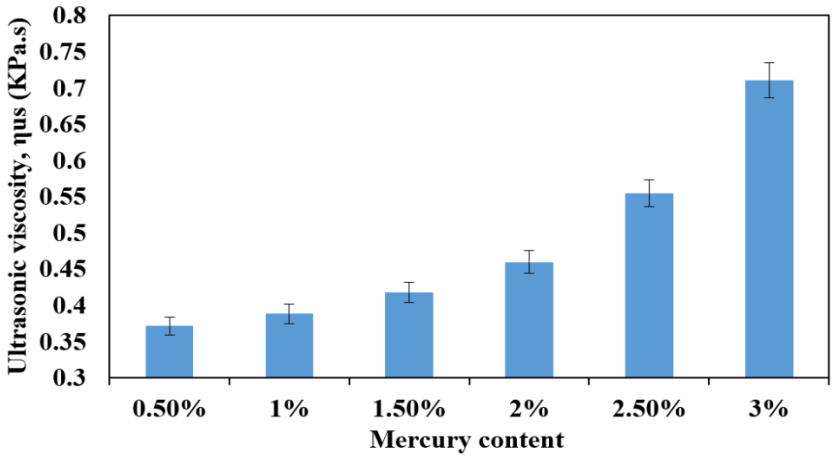

Figure 13: Ultrasonic viscosity for liquid alloys that have different Hg content.

From Figure 13, shows the variation of ultrasonic viscosity with mercury content. It can be inferred from the figure that the ultrasonic viscosity increases from 0.5 to 3 % mercury content. Yehia, Helaly, and El-Sabbagh [32] studied NR-NBR polymer blends using viscosity

measurements. They found that the change in the viscosity of the blend composition showed good linearity. They concluded that the NR-NBR blend system is a semi-compatible blend. Comparing ultrasonic viscosity data in the present study with that obtained by Yehia, Helaly, and El-Sabbagh, one can state that the linear relation between ultrasonic viscosity and mercury content reflects compatibility improvement upon addition of mercury content. The maximum ultrasonic value (about 0.71 KPa.s) was found at 3 % mercury content.

3.2 The optical constants measurements

The optical constants of the alloy specimens mixed with different mercury contents were determined by adjusting the ellipsometer software at wavelengths from 300 nm to 1000 nm and at a fixed angle of incidence of 75° [33]. The optical constants *n*, *k* of the alloy specimens is shown in Figure 14 (a and b).

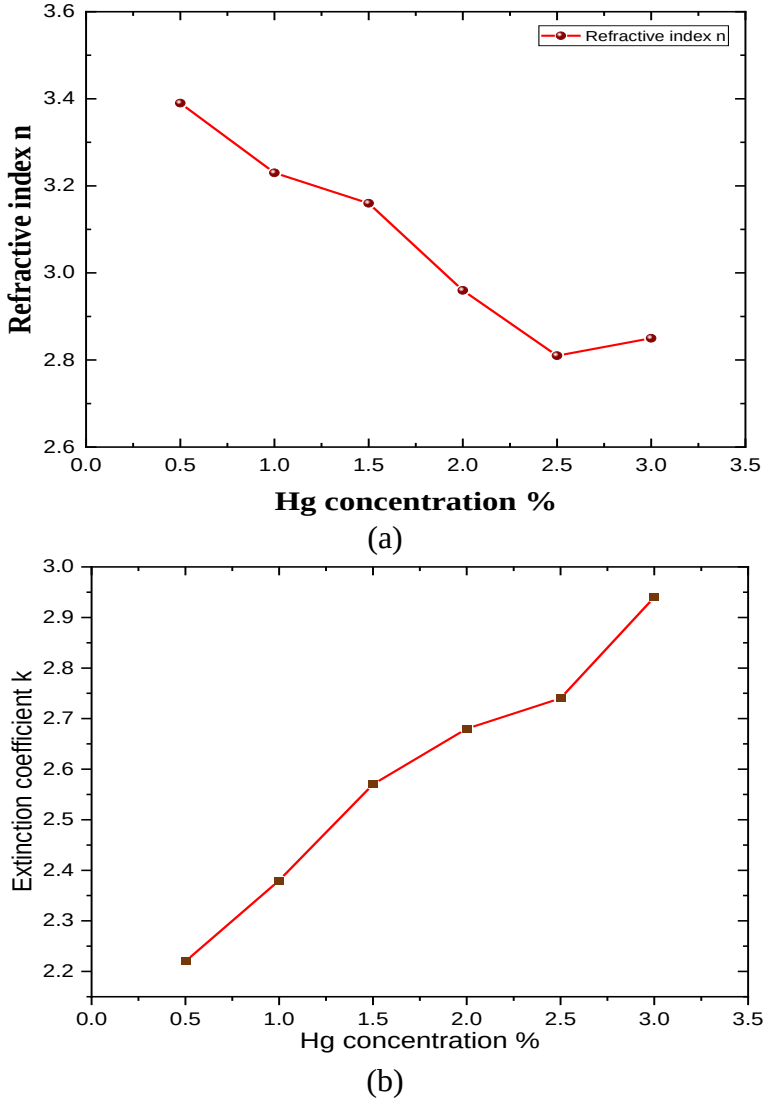

Figure 14: (a) The relation between the refractive index n and the mercury content
(b) The relation between the extinction coefficient k and the mercury content.

The results in Figure 14 indicate a decrease in the refractive index n values with increment of the mercury content of the alloy materials while the extinction coefficient k increased with increasing the percentage of mercury [34]. The refractive index of the material is inversely

proportional with the longitudinal velocity [35]. So as shown in previous sections, the longitudinal velocity increased with increasing mercury content. This in turn confirms the decrement of the refractive index values with increasing the mercury concentration in the alloy materials.

3.2.1 The roughness measurements

The surface roughness was determined using the ellipsometer analysis software and it is represented in Figure 15 [35].

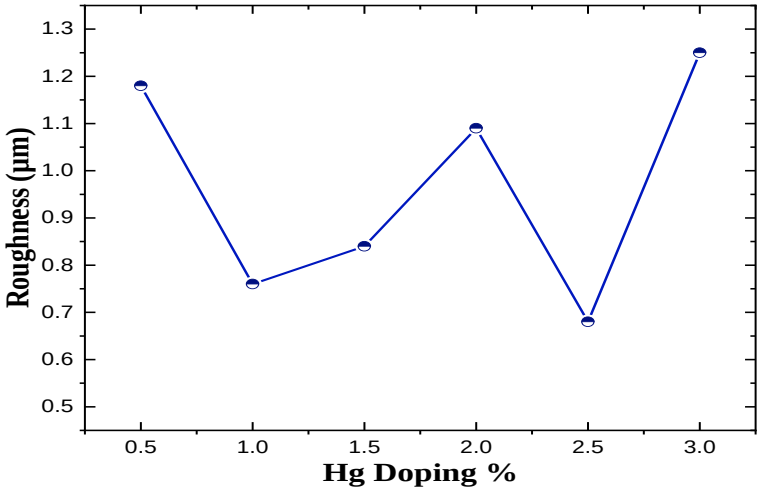

Figure 15: Roughness measurements at different mercury content.

The surface roughness is defined as a homogeneous layer of optical constants composed of a mixture (or combination?) between the optical constants of the two media separating the rough interface. From Figure 15, the surface roughness measured for the alloy specimens ranged from 0.53 µm to 1.26 µm. Thus, some mercury concentrations (0.5, 2, and 3 %) caused increment in the alloy's roughness. While, other mercury concentrations (1, 1.5, and 2.5 %) caused decrement in the alloy's roughness. The increment in the roughness could be due to the presence of defects or impurities in the band structure of the alloy specimens. In the other hand, the decrement of the roughness indicates that the surface is well-arranged without defects or impurities. Therefore, we can say that alloy specimens of mercury content 1, 1.5, and 2.5 % are well- prepared alloy specimens that fulfilled the requirements of preparing suitable reference restorative materials.

3.2.2 Band gap energy

The band gap energy of a material is the energy needed to excite an electron from the valence band to the conduction band. The band gap energy can be determined using the Tauc relation [11] as follows:

$$\alpha h\nu = A\,(h\nu - E_g)^2 \quad (14)$$

$$(\alpha h\nu)^{0.5} = h\nu - E_g \quad (15)$$

Where: E_g is the band gap energy, $(h\nu)$ is the photon energy, and α is the absorption coefficient. The absorption coefficient is related to the extinction coefficient value as illustrated in the following formula:

$$\alpha = 4.\pi.k \text{ / Incident wavelength (nm)} \quad (16)$$

Once the extinction coefficient values are extracted, the absorption coefficients are derived from k values. A plot of the change of the absorption coefficient values with the photon energy for the alloy specimens is illustrated in Figure 16.

The band gap energy can be extracted by plotting a curve between $(\alpha h\nu)^{0.5}$and photon energy $h\nu$. A straight line is obtained as illustrated in Figure 17 (a). The band gap value for each curve E_g is corresponding to the intercept of the linear fitting line with the photon energy axis [11]. The effect of the increment in the mercury content on the band gap energy of the alloy materials has been evaluated and represented in Figure 17 (b). From the figure, the bandgap energy decreased with increasing the mercury content. The band gap is the region between the valence and the conduction bands and has no allowed states. The density of the energy gap and the allowed states depend on the composition of the material. Due to adding mercury to the alloy materials, the chemical composition of the alloy material changed, and new bonds were created in the band gap between the valence and conduction bands. As the mercury density increased, the new bonds converted to molecular orbitals [35]. This yields a reduction in the gap in the interatomic structure of the alloy material, so the band gap of the mercury material will be narrower than that of pure alloy material. A low band gap implies higher intrinsic conduction which means that it will increase the conductivity of the material.

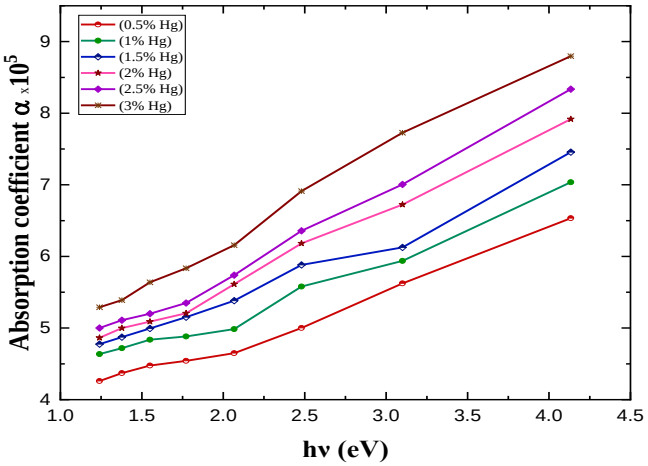

Figure 16: The absorption coefficient values versus the photon energy for different mercury content.

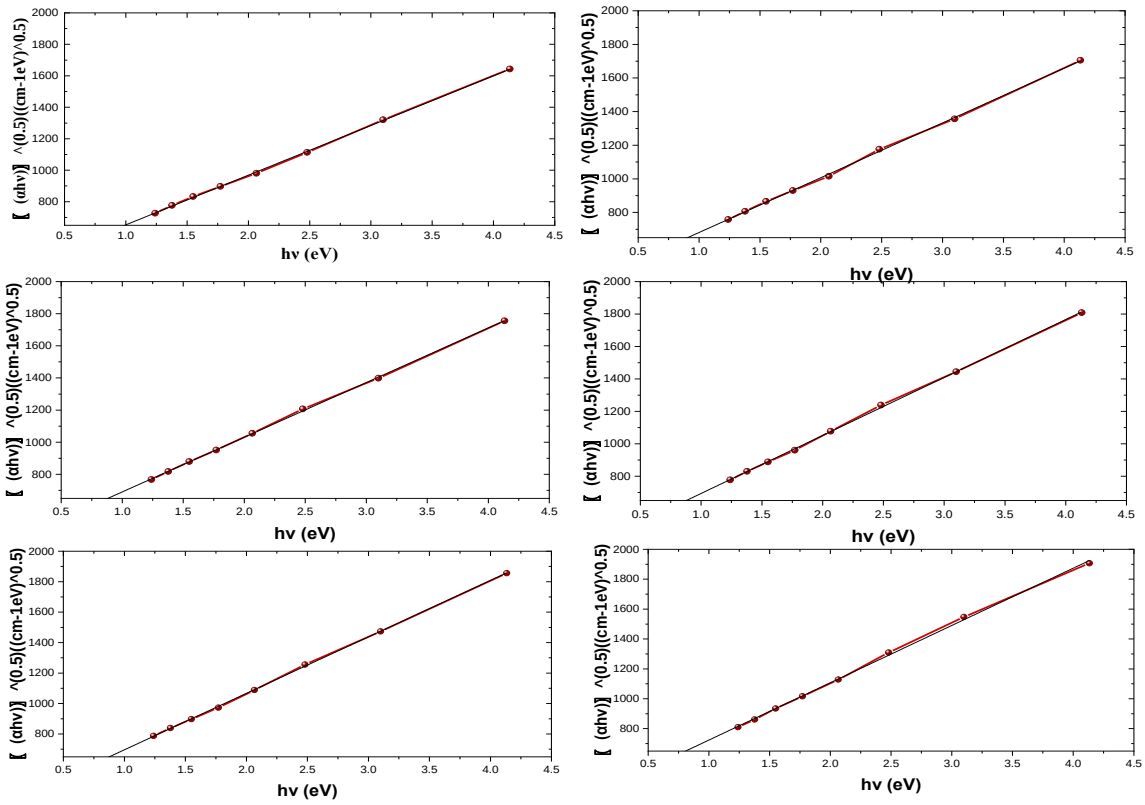

(a)

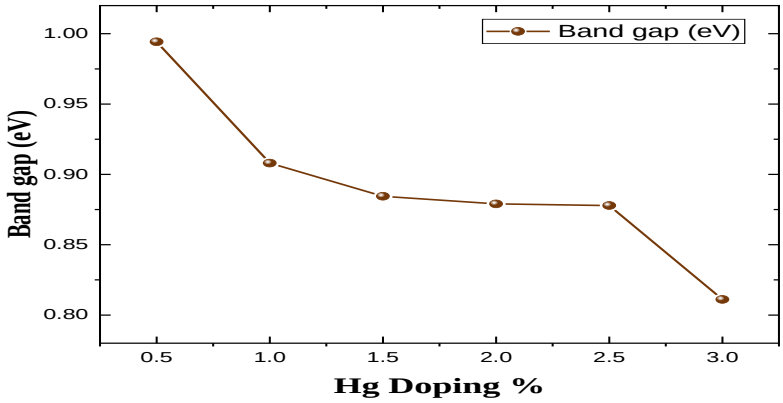

(b)

Figure 17: (a) Relation between $(\alpha h\nu)^{0.5}$ and photon energy $(h\nu)$
(b) the band gap energy relation with mercury content.

3.2.3 Urbach energy

Urbach energy E_u is used to quantify the structure disorder in the band edges of a material that is produced from the defect's existence between the valence and the conduction bands. Due to the fluctuation that occurs as a result of the structural disorder, new energy levels could appear in the forbidden gap of the semiconductor system; this energy level is known as the Urbach tail state. Urbach energy can be obtained from the Urbach empirical rule as follows [11]:

$$\alpha = \alpha_0 \, exp\,(h\nu/E_u) \tag{14}$$

Where: E_u is the Urbach energy, α is the absorption coefficient, and α_0 is a constant.

We take the algorithm from this relation. Then a relation between the algorithm of absorption coefficient as a function of the photon energy is plotted as described in Figure 18 (a). The Urbach energy is evaluated from the slope of the fitting line for each plot in Figure 18 (a). Figure 18 (b) illustrates the relation between the Urbach energy and the mercury content in the alloy specimens.

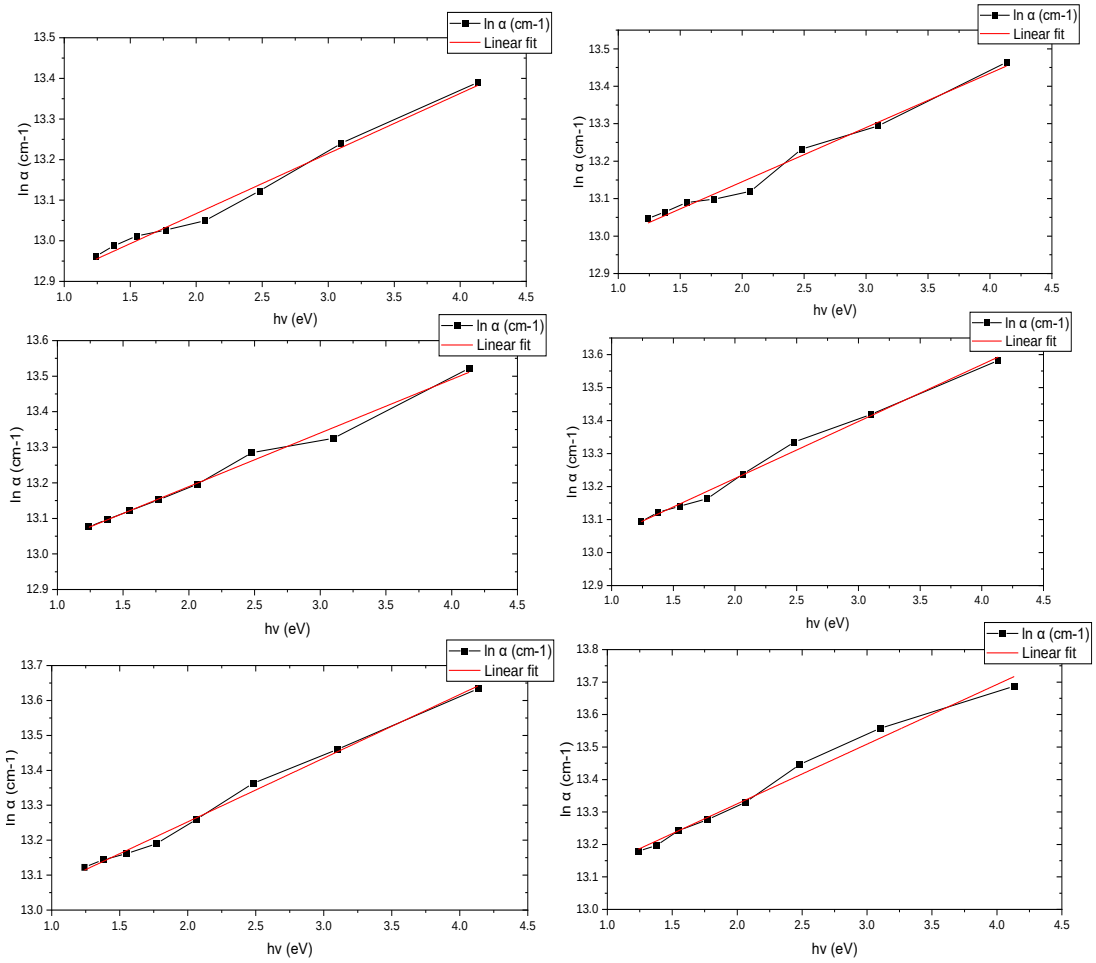

(a)

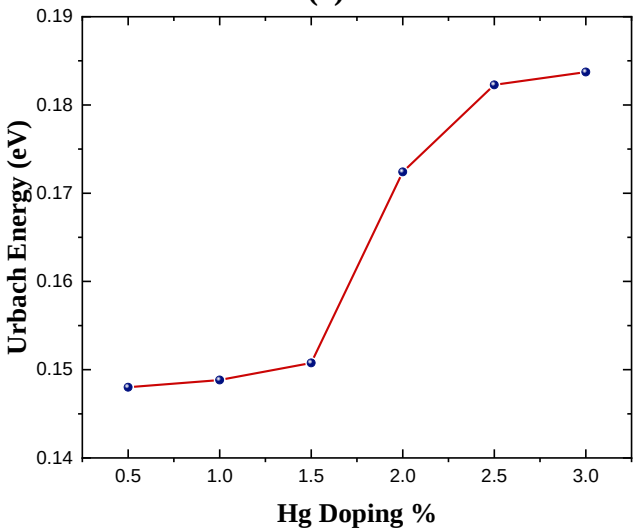

(b)

Figure 18: (a) Relation between ln α and photon energy (hv)
(b) Urbach energy variation with mercury content.

From Figure 18, the Urbach values increased with the mercury content increment. The higher values of Urbach energy yield higher defects between the valence band and the conduction band, lower diffusion lengths of charge carriers, low crystallinity, and large numbers of oxygen vacancies [11]. The alloy specimens of 2, 2.5, and 3 % of mercury had the highest Urbach energy. Therefore, they are the most prepared specimens that have a homogeneous structure that can be used as reference restorative materials.

4 Conclusions

Alloy specimens were prepared, they were composed of platinum modified non-gamma 2 mixed with different mercury percentages (0.5%, 1%, 1.5%, 2%, 2.5% and 3% weight by weight) at room temperature. They had checked their quality, production, and performance repeatability according to a standard to obtain a reference restorative material. In addition, a novel ultrasonic technique was developed to scan the alloy. Poly-methyl-methacrylate delay line was designed to modify the used ultrasonic transducers. The presence of delay line caused reduction in the near field of the used transducers by about 48 %. Thus, the used transducers became more sensitive to (capture?) echoes easily from the specimens. According to standards, the ultrasonic and the optical measurements studied the influence of different content of the mercury in the alloy specimens. Ultrasonic velocities, elastic modulus, Poisson's ration, micro-hardness, attenuation coefficient, and acoustic impedance measurements insured the positive effect of increasing mercury content. Mercury worked to bind all the positively charged metal ions together into a crystal lattice structure. It caused a well-arranged impact alloy structure without gaps or defects. Thus, alloy specimens of high mercury content could be used effectively as pure homogeneous alloy to fabricate reference restorative materials. From the measurements of crosslink density and the ultrasonic viscosity, we deduced that the mercury ions occupy the interstitial space, the interatomic separation decreased, and the alloy's compatibility improved upon increasing the mercury content. The change in the optical constants, absorption coefficient, optical band gap, roughness, and Urbach energy measurements agreed with the ultrasonic results. Finally, when summarizing all results, we can conclude that the alloy specimens of mercury content 1, 1.5, and 2.5 % are good prepared alloy specimens that fulfilled the requirements of preparing suitable reference restorative materials. The specimens with a mercury content of 2.5 % had the most optimum properties.

5 Declarations

5.1 Study Limitations

None.

5.2 Acknowledgements

The authors want to express their deep gratitude to National Institute of Standards – Egypt for supporting this work.

5.3 Funding source

None.

5.4 Competing Interests

There is no conflict of interest exist in this publication.

References

[1] ISO Guide 30 Reference materials-selected terms and definitions. *International Organization for Standardization,* 2015.

[2] Walid Tawfik and Ali Saafan, "Quantitative analysis of mercury in silver dental amalgam alloy using laser induced breakdown spectroscopy with a portable Echelle spectrometer", *International Journal of Pure and Applied Physics* ISSN 0973-1776 Volume 2 Number 3 pp. 195-203, 2006. http://www.ripublication.com/ijpap.htm

[3] Abdalwahid K. Rajih, Kadhim F. Al- Sultani and Manar A. Al- Kinani, "Mechanical Properties Improvement of Dental Amalgam Using TiO2 and ZnO". *Life Sci J*;12(2):86-90 (ISSN:1097-8135), 2015. http://www.lifesciencesite.com.

[4] Barakat, M.A.Y., El-Wakil, A.E.-A.A., Hasan, E.H., "Modification of ultrasonic transducers to study crack propagation in vinyl polymers, supported by SEM technique", *Journal of Vinyl and Additive Technology*, 29(1), pp. 84–99, 2023. DOI:10.1002/vnl.21945

[5] Titiek B. and Ninuk H., "Side effects of mercury in dental amalgam", *Dent. J. (Maj. Ked. Gigi),* Vol. 41. No. 1 January-March: 30-34, 2008. DOI: 10.20473/j.djmkg.v41.i1.p30-34

[6] Hector Jirau-Colón, Leonardo González-Parrilla, Jorge Martinez-Jiménez, Waldemar Adam and Braulio Jiménez-Velez., "Rethinking the Dental Amalgam Dilemma: An Integrated Toxicological Approach", *Int. J. Environ. Res. Public Health*, 16(6), 1036, 2019. DOI:10.3390/ijerph16061036

[7] Richardson, G.M., Wilson, R., Allard, D., Purtill, C., Douma, S., Gravière, J., "Mercury exposure and risks from dental amalgam in the US population, post-2000", *Science of The Total Environment*, 409:4257-4268, 2011. DOI: 10.1016/j.scitotenv.2011.06.035

[8] Shraim, A., Alsuhaimi, A., Al-Thakafy, J.T., "Dental clinics: A point pollution source, not only of mercury but also of other amalgam constituents", *Chemosphere*, 84:1133-1139, 2011. https://doi.org/10.1016/j.chemosphere.2011.04.034

[9] H. G. Tompkins, E. A. Irene, "Handbook of ellipsometry", *Springer-Verlag GmbH,* ISBN: 978-0-8155-1499-2, 2005.

[10] A. W. Abdallah, M. Abdelwahab, "A modified method for calibration of polarimetric components using polarizing interferometry", *Meas. Sci. Technol.*, 32, 115003, 2021. https://doi.org/10.1088/1361-6501/ac0fa7

[11] Al-Shomar, S.M., Barakat, M.A.Y., Abdallah, A.W., "Ellipsometric and ultrasonic studies of nano titanium dioxide specimens doped with Erbium", *Materials Research Express*, 7, 1-13, 2020. DOI:10.1088/2053-1591/abc0d0

[12] ISO 24234:2021 Dentistry – Dental amalgam, 2021.

[13] ASTM E114-15, "Standard Practice for Ultrasonic Pulse-Echo Straight-Beam Contact Testing", *ASTM International,* West Conshohocken, PA, www.astm.org., 2015.

[14] Barakat, M.A.Y., El-Wakil, A.A., "Preparation of polyvinyl acetate composite as a new backing material for the manufacture of ultrasonic transducers", *Journal of Materials Research*, 38(3), pp. 894–905, 2023. DOI:10.1557/s43578-022-00881-y

[15] Vivek T. Rathod., "A Review of Acoustic Impedance Matching Techniques for Piezoelectric Sensors and Transducers", *Sensors*, 20, 4051, 2020. DOI: 10.3390/s20144051

[16] M. A. Y. Barakat, "Amelioration of ultrasonic transducer to study CuO doped thin films", *Arch. Acoust.*, 43(3) 487-495, 2018. DOI:10.24425/123920

[17] P. H. Lissberger, "Ellipsometry and Polarized Light", *Nature*, 269, 270, 1977. https://doi.org/10.1038/269270a0

[18] J. W. Weber1, V. E. Calado, and M. C. M. van de Sanden, "Optical constants of graphene measured by spectroscopic ellipsometry", *Appl. Phys. Lett.*, 97, 091904, 2010. DOI: 10.1063/1.3475393

[19] Barakat M A Y, "Ultrasonic Inspection of Composite Resin Restorative Materials", *International Journal of Engineering & Technology IJET-IJENS*, 14 (3): 1-5, 2014.

[20] Barakat, M.A.Y., "Fabrication of metal–polymer matching layers to improve some ultrasonic transducers for NDT and calibration", *Journal of Materials Science: Materials in Electronics*, 34(12), 1031, 2023. DOI:10.1007/s10854-023-10458-y

[21] Mirham A Y Barakat and Abd El-Aziz A El-Wakil, "Preparation and characterization of EVA/ZnO composites as piezoelectric elements for ultrasonic transducers", Mater. Res. Express 8, 105304, 2021.DOI:10.1088/2053-1591/ac29fb

[22] Giovanni Maizza, Antonio Caporale, Christian Polley and Hermann Seitz; "Micro-Macro Relationship between Microstructure, Porosity, Mechanical Properties, and Build Mode Parameters of a Selective-Electron-Beam-Melted Ti-6Al-4V Alloy"; *Metals*, 9, 786, 2019. DOI:10.3390/met9070786

[23] G. N. Greaves, A. L. Greer, R. S. Lakes & T. Rouxel, "Poisson's ratio and modern materials", *Nature Mater*, 10, 823–837, 2011. https://doi.org/10.1038/nmat3134

[24] Shaoyun F., Zheng S., Pei H., Yuanqing L., Ning H., "Some basic aspects of polymer nanocomposites: A critical review", *Nano Materials Science*, 1: 2–30, 2019. https://doi.org/10.1016/j.nanoms.2019.02.006

[25] Kanji O. A, "Comprehensive Report on Ultrasonic Attenuation of Engineering Materials, Including Metals, Ceramics, Polymers, Fiber-Reinforced Composites, Wood, and Rocks", *Appl. Sci.*, 10(7), 2230, 2020. DOI:10.3390/app10072230

[26] Xu Limei, Cao Jianfang and Huang Dagui, "Design and Characterization of a PVDF Ultrasonic Acoustic Transducer Applied in Audio Beam Loudspeaker", *Proceedings of the IEEE International Conference on Mechatronics & Automation Niagara Falls*, Canada, 2005. DOI: 10.1109/ICMA.2005.1626868

[27] Hiremath, N., et al., "An Overview of Acoustic Impedance Measurement Techniques and Future Prospects", *Metrology*, 1(1): 17-38, 2021. DOI:10.3390/METROLOGY1010002

[28] Maamoun, A.A., Barakat, M.A.Y., El-Wakil, A.E.-A.A., Zulfiqar, S., Oghenekohwo, V.J., "Valorization of eggshell waste in designing flexible polyurethane-based piezoelectric composite materials for ultrasonic transducers", *Journal of Polymer Research*, 30(7), 286, 2023. DOI:10.1007/s10965-023-03648-z

[29] W. Weglewski, K. Bochenek, M. Basista, T. Schubert, U. Jehring, J. Litniewski, S. M arkiewicz, "Comparative assessment of Young's modulus measurements of metal-ceramic composites using mechanical and non-destructive tests and micro-CT based

computational modelling", *Comput. Mater. Sci.*, 77, pp. 19-30, 2013. DOI:10.1016/j.commatsci.2013.04.007

[30] Rymantas Kazys and Regina Rekuviene, "Viscosity and density measurement methods for polymer melts", ISSN 1392-2114 *ULTRAGARSAS (ULTRASOUND),* Vol. 66, No. 4, 2011. https://www.ndt.net/?id=11878

[31] Barakat, M.A.Y., El-Sabbagh, S.H., Mohamed, W.S., Mahmoud, D.S., "Nanoarchitectonics of ethylene propylene diene monomer (EPDM) composites reinforced with Cu–Al–Zn-alloy for ultrasonic array transducers' fabrication", *Applied Physics A: Materials Science and Processing*, 129(6), 422, 2023. DOI:10.1007/s00339-023-06688-w

[32] Yehia, A.A., Mansour, A.A. & Stoll, B., "Detection of compatibility of some rubber blends by DSC", *Journal of Thermal Analysis*, 48, 1299–1310, 1997. https://doi.org/10.1007/BF01983440

[33] A. W. Abdallah, M. Abdelwahab, M., M. El-Bahrawy, "Developed method to evaluate some optical parameters in gauge block measurements using ellipsometry", *MAPAN*, 37(2), 319–328, 2022. https://doi.org/10.1007/s12647-021-00521-6

[34] Abou Hussein, E.M., Barakat, M.A.Y., "Structural, physical and ultrasonic studies on bismuth borate glasses modified with Fe2O3 as promising radiation shielding materials", *Materials Chemistry and Physics*, 290,126606, 2022. DOI: 10.1016/j.matchemphys.2022.126606

[35] M. A. Y. Barakat, M. Abdelwahab, A. W. Abdallah, "Evaluation of new designed reference blocks for calibration and NDT by optical and ultrasonic techniques", Metrology and Measurement Systems, 29, 4, 719 – 736, 2022. DOI:10.24425/mms.2022.143072